

Electron-Transfer Kinetics of Zn-Substituted Cytochrome *c* and Its Ru(NH₃)₅(Histidine-33) Derivative

Horst Elias,[†] Mei H. Chou, and Jay R. Winkler*

Contribution from the Department of Chemistry, Brookhaven National Laboratory, Upton, New York 11973. Received May 11, 1987

Abstract: The kinetics of the bimolecular electron transfers from triplet-excited zinc-substituted horse heart cytochrome *c* (Zn-cyt *c*^{*}) to Ru(NH₃)₅L³⁺ have been measured (L = NH₃, $k(298\text{ K}) = 1.4 \times 10^7\text{ M}^{-1}\text{ s}^{-1}$; L = histidine, $k(298\text{ K}) = 2.4 \times 10^7\text{ M}^{-1}\text{ s}^{-1}$), along with those of the corresponding thermal back-reactions (L = NH₃, $k(298\text{ K}) = 1.5 \times 10^8\text{ M}^{-1}\text{ s}^{-1}$; L = histidine, $k(298\text{ K}) = 3.6 \times 10^8\text{ M}^{-1}\text{ s}^{-1}$). The derivatized metalloprotein ruthenium pentaammine histidine-33-zinc-substituted cytochrome *c* (Ru-Zn-cyt *c*) has been prepared and characterized by atomic absorption spectroscopy and HPLC analysis of its tryptic digestion fragments. The rate of intraprotein electron transfer from the triplet-excited Zn-porphyrin moiety to the 11.8-Å distant Ru(NH₃)₅(His-33)³⁺ residue ($k(298\text{ K}) = 7.7 \times 10^5\text{ s}^{-1}$), as well as that of the thermal back-reaction ($k(298\text{ K}) = 1.6 \times 10^6\text{ s}^{-1}$), has been measured by transient spectroscopy. Intraprotein electron transfer from Ru(II) quenches Zn-cyt *c*^{*} with a rate constant of $2.4 \times 10^2\text{ s}^{-1}$. These kinetics are discussed in terms of the semiclassical theory of electron-transfer reactions.

The experimental separation of diffusion from activated processes in electron-transfer reactions is of central importance in identifying the barriers for each step. A particularly successful method of achieving this separation has involved the study of electron-transfer reactions between redox centers that are held at fixed distance and orientation. Three approaches have been applied to fixed-site electron-transfer reactions in metalloproteins: studies of (1) protein-protein¹⁻⁴ and protein-small molecule ion pairs,⁵ (2) native and hybrid multisite proteins,⁶ and (3) synthetic multisite proteins.⁷⁻¹³ A new synthetic multisite protein has been prepared, and the kinetics of three of its intraprotein electron-transfer reactions form the subject of this report.

In 1982 Gray and co-workers first reported the synthesis^{7a} of the multisite protein ruthenium pentaammine histidine-33-ferricytochrome *c* (Ru-Fe-cyt *c*) and the kinetics^{7b,c} of the intraprotein electron transfer from Ru(II) to Fe(III) ($k = 30$ (3) s⁻¹, 23 °C). Several more synthetic multisite proteins have since been prepared by coordination of ruthenium ammine groups to histidine residues of a variety of native metalloproteins.⁸⁻¹³ Measurements of rates of intraprotein electron transfer in these systems have contributed to a growing body of data on fixed-site electron-transfer kinetics in metalloproteins.

We have prepared a variant of the above synthetic multisite protein by coordinating ruthenium pentaammine to histidine-33 of zinc-substituted cytochrome *c* (Ru-Zn-cyt *c*). The importance of Ru-Zn-cyt *c* in the study of electron transfer derives from the photophysical properties of Zn-cyt *c*. The lowest energy triplet excited state of Zn-cyt *c* lies 1.7 eV above the ground state¹⁴ and has a lifetime of 15 ms at room temperature.¹⁵ In this triplet excited state, the Zn-porphyrin moiety is able to reduce a Ru(NH₃)₅(His)³⁺ complex and oxidize the corresponding Ru(II) species. In principle, then, Ru-Zn-cyt *c* can be used to measure four fixed-site electron-transfer rates: the reductive and oxidative quenching of excited Zn-cyt *c* by the Ru(II)- and Ru(III)-pentaammine His-33 complexes, respectively, and the two corresponding thermal back-reactions. Three of these four electron-transfer rates have been measured by flash photolysis techniques and, along with corresponding bimolecular kinetics, are described below.

Experimental Section

Materials. All aqueous solutions were prepared with house distilled water that had been further purified by passage through a Millipore Q3 water purification system. Sodium phosphate (NaP_i) buffers were prepared from analytical-grade reagents. HEPES (Sigma Chemical Co.) buffers were prepared from solutions of the free acid by adjusting the pH with 10 M NaOH. Horse heart cytochrome *c*, type VI, and trypsin from

bovine pancreas, type XIII (TPCK treated), were supplied by the Sigma Chemical Co. When used in its native form, cytochrome *c* was first purified on a CM-cellulose (Watman CM-52) column.¹⁶ L-Histidine (His) (98%, Aldrich Chemical Co.) was used without further purification.

Unless otherwise specified, protein samples were maintained at 4 °C. All manipulations of Zn-cyt *c* samples were performed with the exclusion of room light.

Preparations. Crude Ru(NH₃)₆Cl₃ was obtained from Mathey-Bishop Inc. and purified by the method of Pladziewicz et al.¹⁶ [Ru(NH₃)₅Cl]Cl₂

- (1) Simolo, K. P.; McLendon, G. L.; Mauk, M. R.; Mauk, A. G. *J. Am. Chem. Soc.* **1984**, *106*, 5012-5013.
- (2) (a) McLendon, G. L.; Winkler, J. R.; Nocera, D. G.; Mauk, M. R.; Mauk, A. G.; Gray, H. B. *J. Am. Chem. Soc.* **1985**, *107*, 739-740. (b) McLendon, G. L.; Miller, J. R. *J. Am. Chem. Soc.* **1985**, *107*, 7811-7816.
- (3) (a) Ho, P. S.; Sutoris, C.; Liang, N.; Margoliash, E.; Hoffman, B. M. *J. Am. Chem. Soc.* **1985**, *107*, 1070-1071. (b) Liang, N.; Kang, C. H.; Ho, P. S.; Margoliash, E.; Hoffman, B. M. *J. Am. Chem. Soc.* **1986**, *108*, 4665-4666.
- (4) (a) Cheung, E.; Taylor, K.; Kornblatt, J. A.; English, A. M.; McLendon, G. L.; Miller, J. R. *Proc. Natl. Acad. Sci. U.S.A.* **1986**, *83*, 1330-1333. (b) Conklin, K. T.; McLendon, G. L. *Inorg. Chem.* **1986**, *25*, 4804-4806.
- (5) Brunschwig, B. S.; DeLaive, P. J.; English, A. M.; Goldberg, M.; Gray, H. B.; Mayo, S. L.; Sutin, N. *Inorg. Chem.* **1985**, *24*, 3743-3749.
- (6) (a) McGourty, J. L.; Blough, N. V.; Hoffman, B. M. *J. Am. Chem. Soc.* **1983**, *105*, 4470-4472. (b) Peterson-Kennedy, S. E.; McGourty, J. L.; Kalweit, J. A.; Hoffman, B. M. *J. Am. Chem. Soc.* **1984**, *106*, 5010-5012. (c) Peterson-Kennedy, S. E.; McGourty, J. L.; Kalweit, J. A.; Hoffman, B. M. *J. Am. Chem. Soc.* **1986**, *108*, 1739-1746.
- (7) (a) Yocom, K. M.; Shelton, J. B.; Shelton, J. R.; Schroeder, W. A.; Worosila, G.; Isied, S. S.; Bordignon, E.; Gray, H. B. *Proc. Natl. Acad. Sci. U.S.A.* **1982**, *79*, 7052-7055. (b) Winkler, J. R.; Nocera, D. G.; Yocom, K. M.; Bordignon, E.; Gray, H. B. *J. Am. Chem. Soc.* **1982**, *104*, 5798-5800. (c) Nocera, D. G.; Winkler, J. R.; Yocom, K. M.; Bordignon, E.; Gray, H. B. *J. Am. Chem. Soc.* **1984**, *106*, 5145-5150.
- (8) (a) Isied, S. S.; Worosila, G.; Atherton, S. J. *J. Am. Chem. Soc.* **1982**, *104*, 7659-7661. (b) Isied, S. S.; Kuehn, C.; Worosila, G. *J. Am. Chem. Soc.* **1984**, *106*, 1722-1726. (c) Bechtold, R.; Gardineer, M. B.; Kazmi, A.; van Hemelryck, B.; Isied, S. S. *J. Phys. Chem.* **1986**, *90*, 3800-3804.
- (9) Kostić, N. M.; Margalit, R.; Che, C. M.; Gray, H. B. *J. Am. Chem. Soc.* **1983**, *105*, 7765-7767.
- (10) Crutchley, R. J.; Ellis, W. R.; Gray, H. B. *J. Am. Chem. Soc.* **1985**, *107*, 5002-5004.
- (11) Bechtold, R.; Kuehn, C.; Lepre, C.; Isied, S. S. *Nature (London)* **1986**, *322*, 286-288.
- (12) Mayo, S. L.; Ellis, W. R.; Crutchley, R. J.; Gray, H. B. *Science (Washington, D.C.)* **1986**, *233* 948-952.
- (13) Axup, A. W.; Albin, M.; Mayo, S. L.; Crutchley, R. J.; Gray, H. B., submitted for publication in *J. Am. Chem. Soc.*
- (14) Vanderkooi, J. M.; Adara, F.; Erecińska, M. *Eur. J. Biochem.* **1976**, *64*, 381-387.
- (15) (a) Dixit, B. P. S. N.; Waring, A. J.; Vanderkooi, J. M. *FEBS Lett.* **1981**, *125*, 86-88. (b) Dixit, B. P. S. N.; Moy, V. T.; Vanderkooi, J. M. *Biochemistry* **1984**, *23*, 2103-2107.
- (16) Pladziewicz, J. R.; Meyer, T. J.; Broomhead, J. A.; Taube, H. *Inorg. Chem.* **1973**, *12*, 639-643.

[†] Permanent address: Technische Hochschule Darmstadt, Eduard-Zintl-Institut, 6100 Darmstadt, Federal Republic of Germany.

was prepared from the hexaammine¹⁷ and purified by recrystallization from hot 0.1 M HCl. $[\text{Ru}(\text{NH}_3)_5(\text{His})]\text{Cl}_3$ was prepared by the method of Sundberg and Gupta¹⁸ and purified by recrystallization from ethanol/water. Anal. $(\text{Ru}(\text{NH}_3)_5(\text{His})\text{Cl}_3 \cdot 2\text{H}_2\text{O})$ Ru, Cl.

Zn-cyt *c* was prepared according to the following procedure.¹⁹ Commercial Fe-cyt *c* dissolved in water (0.5 g per ca. 30 mL) was placed in a Teflon bottle and lyophilized. The bottle containing the dried protein was transferred to an all-Teflon gas manifold, and nitrogen gas was passed over the sample for 15 min. The sample was cooled to 77 K, and anhydrous HF (Matheson, further dried by passage through CoF_3) was condensed onto the sample (2–3 mL). The protein sample was thoroughly mixed with the HF and then allowed to warm to room temperature while the HF was removed under a stream of N_2 . The resultant crude H_2 -cyt *c* residue was taken up with 50 mM, pH 5, ammonium acetate (NH_4OAc) at 4 °C. Low molecular weight impurities were removed by ultrafiltration through a 5000-MW cutoff membrane (Watman, YM-5). The concentrated metal-free cyt *c* sample was loaded onto a 2.5×60 cm CM-cellulose (Watman CM-52) column and eluted with 85 mM, pH 7.0, NaP_i . Some minor bands preceded the major band that eluted in a volume of ca. 2000–2400 mL. The fractions containing the major band from the column were concentrated by ultrafiltration and then equilibrated with 50 mM, pH 5, NH_4OAc . The final protein concentration was ca. 0.75 mM. A 15-fold excess of zinc acetate was added, and the solution was heated to 35–40 °C. The reaction was monitored spectrophotometrically,¹⁴ and when complete (ca. 3 h), the excess Zn^{2+} was removed by ultrafiltration. The crude Zn-cyt *c* sample was purified by cation-exchange chromatography (2.5×55 cm CM-52; 85 mM, pH 7.0, NaP_i). The overall yield of purified Zn-cyt *c* ranged from 30 to 40%.

The derivatized protein, $\text{Ru}(\text{NH}_3)_5(\text{His-33})\text{-Zn-cyt } c$, was prepared by the reaction of $\text{Ru}(\text{NH}_3)_5(\text{OH}_2)^{2+}$ with Zn-cyt *c* by a procedure identical with that developed for native Fe-cyt *c*.^{7a,c} The chromatogram of the reaction products was quite similar to that reported for the ruthenium modification of the native protein. The band containing Ru-Zn-cyt *c* was further purified by at least one additional pass down a 2.5×25 cm CM-52 column (100 mM, pH 7.0, NaP_i). In order to ensure the highest possible sample purity, only the central fractions of the chromatography band were used in subsequent experiments. The metal content of the protein sample was analyzed by atomic absorption spectroscopy, and the ratio of Ru to Zn was found to be 1:1, within 10%.

Methods. Tryptic digestions were performed according to the method described by Yocom et al.,^{7a} and virtually identical conditions were used for the HPLC analysis. A Perkin-Elmer Series 2 liquid chromatograph was used in conjunction with a Perkin-Elmer LC-85 spectrophotometric detector. The column used was a 4.6 mm \times 25 cm Beckman Ultrasphere ODS with a 5- μm particle size. The flow rate was 1 mL/min, with a linear gradient starting from 3% acetonitrile and 97% 50 mM potassium phosphate (pH 2.85) and increasing the acetonitrile concentration at a rate of 0.4%/min. The chromatograms ($\lambda_{\text{obsd}} = 225$ nm) of the tryptic digestion fragments from Fe-cyt *c* and Zn-cyt *c* were essentially identical, except in the region of the porphyrin-containing fragment (supplementary material Figure 1). The chromatogram of the tryptic digestion fragments from Ru-Zn-cyt *c* showed one major and one minor peak shifted from those of Zn-cyt *c*. The shifted peaks appeared in nearly the same elution volume as that reported for the two T7 fragments of Ru-Fe-cyt *c*.^{7a} Both shifted peaks appeared when the chromatogram was monitored at 300 nm and are the only peaks that are not also present in the 300-nm chromatogram of the Zn-cyt *c* fragments (supplementary material Figure 2). Online spectra were recorded for the two peaks, and both spectra matched that of $\text{Ru}(\text{NH}_3)_5(\text{His})^{3+}$ (supplementary material Figure 3). The two peaks very likely correspond to two different cleavage sites for the fragment containing histidine-33. Similar results were reported for Ru-Fe-cyt *c*.

Triplet decay and electron-transfer kinetics were measured by flash transient spectroscopy. The excitation source was a mode-locked, frequency-doubled Nd:YAG laser, which has been described elsewhere.²⁰ Kinetics data were averages of at least 25 laser excitation pulses, and the samples were gently stirred between laser shots. Samples were held in 1-cm path length cuvettes and were exhaustively deoxygenated by repeated evacuation/back-fill cycles using purified Ar gas. The solvent used for all kinetics measurements was $\mu = 0.1$ M, pH 7.0, NaP_i .

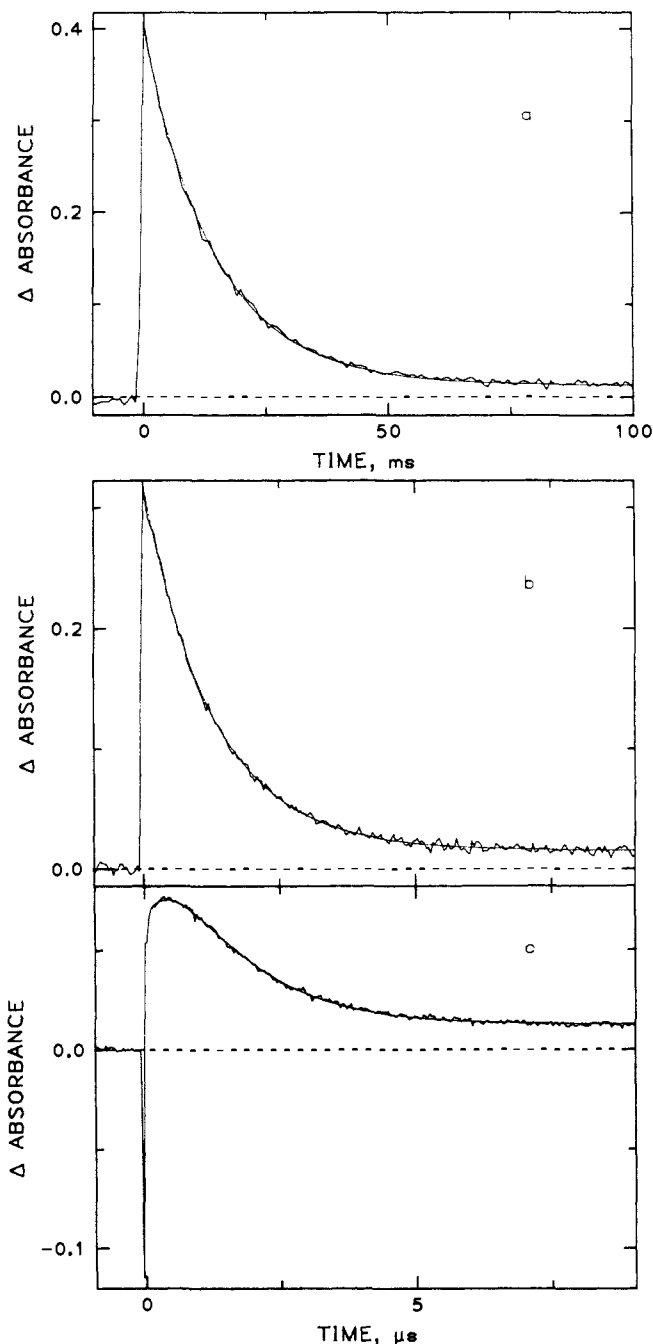


Figure 1. Transient kinetics of Zn-cyt *c* and Ru(III)-Zn-cyt *c* produced by 30-ps, 532-nm excitation of $(1.5\text{--}2) \times 10^{-5}$ M samples in 1-cm cuvettes. Zn-cyt *c*: (a) $\lambda_{\text{obsd}} = 450$ nm, smooth curve through the data is a single exponential decay function with a rate constant of 68 s^{-1} . Ru(III)-Zn-cyt *c*: (b) $\lambda_{\text{obsd}} = 450$ nm, smooth curve is a single exponential function with a rate constant of $7.70 \times 10^5 \text{ s}^{-1}$; (c) $\lambda_{\text{obsd}} = 675$ nm, smooth curve is a biexponential function with rate constants of 1.65×10^6 and $7.70 \times 10^5 \text{ s}^{-1}$.

Results

Preparation of Ru-Zn-cyt *c*. The reaction between $\text{Ru}(\text{NH}_3)_5(\text{OH}_2)^{2+}$ and Zn-cyt *c* and subsequent workup were essentially identical with those of the native protein.^{7a} Elemental analysis of the desired fraction revealed a 1:1 ratio between Ru and Zn. The tryptic digestion and HPLC analysis of Ru-Zn-cyt *c* were also quite similar to those of the Fe-containing protein. Especially convincing evidence of the His-33 derivatization is provided by the absorption spectrum of the Ru-containing peptide fragment from the tryptic digestion, which was identical with that of $\text{Ru}(\text{NH}_3)_5(\text{His})^{3+}$. The atomic absorption and HPLC analyses strongly support the conclusion that the modified protein is indeed $\text{Ru}(\text{NH}_3)_5(\text{His-33})\text{-Zn-cyt } c$.

(17) Lawrence, G. A.; Lay, P. A.; Sargeson, A. M.; Taube, H. *Inorg. Synth.* **1986**, *24*, 258.

(18) Sundberg, R. J.; Gupta, G. *Bioinorg. Chem.* **1973**, *3*, 39–48.

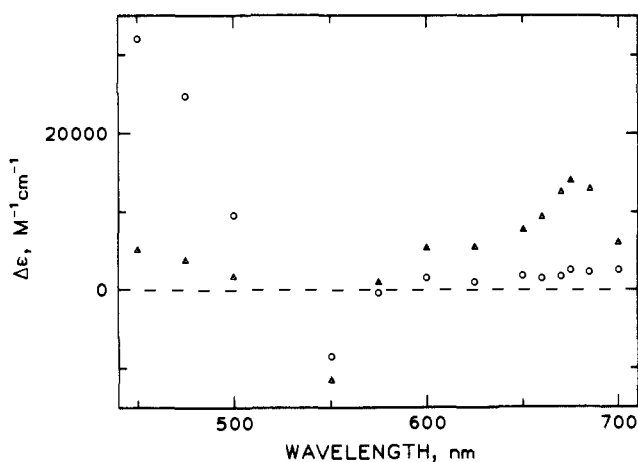
(19) (a) Fisher, W. R.; Taniuchi, H.; Anfinsen, C. B. *J. Biol. Chem.* **1973**, *248*, 3188–3195. (b) Vanderkooi, J. M.; Erecińska, M. *Eur. J. Biochem.* **1975**, *60*, 199–207.

(20) (a) Winkler, J. R.; Nocera, D. G.; Netzel, T. L. *J. Am. Chem. Soc.* **1986**, *108*, 4451–4458. (b) Winkler, J. R.; Netzel, T. L.; Creutz, C.; Sutin, N. *J. Am. Chem. Soc.* **1987**, *109*, 2381–2392.

Table I. Observed and Calculated Rate Constants and Activation Parameters for the Bimolecular Reactions of Ru(NH₃)₅L³⁺ (L = NH₃, His; *n* = 2, 3) with M-Cyt *c* (M = Fe, Zn)

no.	reaction	$-\Delta G^\circ$, eV	$k_{\text{obsd}}(298 \text{ K})$, M ⁻¹ s ⁻¹	E_a , kcal mol ⁻¹	ΔS^\ddagger , ^a eu	$k_{\text{calcd}}(298 \text{ K})$, ^b M ⁻¹ s ⁻¹
1	Ru(NH ₃) ₆ ²⁺ + Fe(III)-cyt <i>c</i> ^c	0.20 (1)	6.7 (1) × 10 ⁴	1.5 (2)	-33 (1)	1.2 × 10 ⁵
2	Ru(NH ₃) ₅ (His) ²⁺ + Fe(III)-cyt <i>c</i> ^c	0.18 (1)	8.5 (1) × 10 ⁴	0.8 (2)	-35 (1)	8.4 × 10 ⁴
3	Ru(NH ₃) ₆ ²⁺ + Zn-cyt <i>c</i> ⁺⁺	0.84 (10)	1.5 (2) × 10 ⁸	3.2 (4)	-11 (2)	1.4 × 10 ⁸
4	Ru(NH ₃) ₅ (His) ²⁺ + Zn-cyt <i>c</i> ⁺⁺	0.82 (10)	3.6 (5) × 10 ⁸			1.2 × 10 ⁸
5	Zn-cyt <i>c</i> ⁺ + Ru(NH ₃) ₆ ³⁺	0.86 (10)	1.4 (1) × 10 ⁷	3.3 (4)	-16 (2)	1.6 × 10 ⁸
6	Zn-cyt <i>c</i> ⁺ + Ru(NH ₃) ₅ (His) ³⁺	0.88 (10)	2.4 (3) × 10 ⁷	2.4 (3)	-18 (2)	1.7 × 10 ⁸

^aThe activation entropy ΔS^\ddagger is related to the Arrhenius preexponential factor A through the relation $\Delta S^\ddagger = R \ln(A/\nu)$, $\nu = 1 \times 10^{13} \text{ s}^{-1}$. ^bRates were calculated with eq 1-6 with $\lambda = 1.2 \text{ eV}$ and $\ln(\nu K_A) = 19.8$. ^cReference 7c.

**Figure 2.** Molar difference spectra of Zn-cyt *c*^{*}/Zn-cyt *c* (○) and Zn-cyt *c*⁺/Zn-cyt *c* (△).

Bimolecular Kinetics. The triplet excited state of Zn-cyt *c* (Zn-cyt *c*^{*}) decays exponentially at 25 °C in $\mu = 0.1 \text{ M}$ buffer with a rate constant $k_0 = 68 \text{ s}^{-1}$ (Figure 1a).^{21a} The decay rate is virtually independent of temperature between 5 and 35 °C and then begins to increase at higher temperatures. Plots of $\ln k_0$ vs T^{-1} are approximately linear for temperatures below 40 °C and yield the Arrhenius parameters $E_a = 0.8 \text{ kcal mol}^{-1}$ and $A = 2.8 \times 10^2 \text{ s}^{-1}$.

The Zn-cyt *c* triplet excited state is quenched in the presence of the electron acceptors Ru(NH₃)₅L³⁺ (L = NH₃, His). Under these conditions the triplet does not decay back to the ground state but instead yields another product that subsequently decays back to the starting material. The two likely mechanisms for Zn-cyt *c*^{*} quenching by Ru(NH₃)₅L³⁺ are energy transfer and electron transfer. Since the lifetimes of the low-lying excited states of Ru(NH₃)₅L³⁺ are expected to be extremely short (<10 ns²²), the observed products of the quenching reaction must be the electron-transfer products, Zn-cyt *c*⁺⁺ and Ru(NH₃)₅L²⁺. The spectrum of Ru(NH₃)₆²⁺ has no strong absorption bands in the visible region,²³ so the difference spectrum recorded for the products of Ru(NH₃)₆³⁺ quenching will correspond to the difference spectrum between Zn-cyt *c*⁺⁺ and Zn-cyt *c*. This difference spectrum is shown in Figure 2 along with the Zn-cyt *c*^{*}/Zn-cyt *c* difference spectrum. The method of estimating the molar absorptances of the two transient species will be described below. The important feature that these spectra reveal is that while 450 nm is a good wavelength for detecting the Zn-cyt *c* triplet, it is a poor wavelength for observing the cation radical. The cation radical produced from the triplet is best detected at 675 nm because at

this wavelength the molar absorptance of Zn-cyt *c*⁺⁺ exceeds that of Zn-cyt *c*^{*} by the greatest amount (in the 450–700-nm spectral range).

Stern–Volmer plots of $\ln\{[k([\text{Ru(III)})] - k_0] / [\text{Ru(III)}]\}$ vs $[\text{Ru(III)}]$ for quenching Zn-cyt *c*^{*} by Ru(NH₃)₅L³⁺ (L = NH₃, His) are linear between 10⁻⁴ and 10⁻² M $[\text{Ru(III)}]$. The bimolecular rate constants for the quenching reactions, along with corresponding Arrhenius parameters determined at $[\text{Ru(III)}] = 10^{-3} \text{ M}$, are shown in Table I. Kinetics data for the back electron transfer from the Ru(II)–ammine complexes to Zn-cyt *c*⁺⁺ also appear in Table I. The bimolecular rate constant and activation parameters for the back electron transfer from Ru(NH₃)₆²⁺ were determined from the pseudo-first-order decay of Zn-cyt *c*⁺⁺ produced by flashing a solution containing Zn-cyt *c* ($1.5 \times 10^{-5} \text{ M}$), Ru(NH₃)₆³⁺ (10^{-2} M), and Ru(NH₃)₆²⁺ (10^{-4} M). This value for the back-reaction rate constant was then used to fit the kinetics of the back-reaction between Zn-cyt *c*⁺⁺ and Ru(NH₃)₆²⁺ to a second-order decay function. This fit yields an estimate for the molar absorptance of Zn-cyt *c*⁺⁺ at 675 nm, $\epsilon_{675}(\text{Zn-cyt } c^{++}) = 1.40 (5) \times 10^4 \text{ M}^{-1} \text{ cm}^{-1}$. The molar difference spectrum of Zn-cyt *c*⁺⁺/Zn-cyt *c* follows directly from this measurement. Given this molar absorptivity, the rate constant of the back-reaction between Zn-cyt *c*⁺⁺ and Ru(NH₃)₅(His)²⁺ was determined from a second-order fit to the back-reaction kinetics (Table I).

In order to evaluate the yield of electron-transfer products in the bimolecular quenching of Zn-cyt *c*^{*} by Ru(NH₃)₅L³⁺, the molar difference spectrum for Zn-cyt *c*^{*}/Zn-cyt *c* had to be determined. A lower limit to the molar absorptivity of Zn-cyt *c*^{*} was provided by saturation of the 450-nm triplet signal of a 4.8 μM Zn-cyt *c* solution. The maximum absorbance change was $\Delta A_{450}(1 \text{ cm}) = 0.138 (2)$, leading to the estimate $\Delta \epsilon_{450}(\text{Zn-cyt } c^*/\text{Zn-cyt } c) = 2.9 (1) \times 10^4 \text{ M}^{-1} \text{ cm}^{-1}/\Phi_f$, where Φ_f is the quantum yield for formation of Zn-cyt *c*^{*}. With $\Phi_f = 0.9$ for Zn-cyt *c*,^{15b} it can be concluded that $\Delta \epsilon_{450}(\text{Zn-cyt } c^*/\text{Zn-cyt } c) = 3.2 (1) \times 10^4 \text{ M}^{-1} \text{ cm}^{-1}$. Under conditions of complete Zn-cyt *c*^{*} quenching ($[\text{Ru(NH}_3)_6^{3+}] = 0.1 \text{ M}$), the ratio of the initial triplet signal at 450 nm to that of the radical at 675 nm is $\Delta A_{450}(\text{Zn-cyt } c^*/\text{Zn-cyt } c)/\Delta A_{675}(\text{Zn-cyt } c^*/\text{Zn-cyt } c) = 5.5$, indicating that the yield of cage-escaped electron-transfer products is ca. 0.4. There are two likely origins for the less than 100% yield of separated electron-transfer products: rapid geminate recombination and energy transfer. The electron-transfer cage-escape yield for Ru(NH₃)₅(His)³⁺ quenching is about 0.25, indicating either faster geminate recombination or more efficient energy transfer than that which occurs with Ru(NH₃)₆³⁺.

Unimolecular Kinetics. The triplet state of Ru(III)–Zn-cyt *c* decays with a first-order rate constant of $7.7 (2) \times 10^5 \text{ s}^{-1}$ (25 °C) that is independent of protein concentration between 2×10^{-6} and $2 \times 10^{-5} \text{ M}$ (Figure 1b).^{21b} The greater than 10⁴-fold increase in triplet decay rate as compared to the unmodified protein demonstrates that the presence of the Ru(NH₃)₅(His-33)³⁺ residue introduces an efficient nonradiative decay pathway. Between 5 and 55 °C the triplet decay rate increases by less than a factor of 2. Arrhenius plots of $\ln k_{\text{obsd}}$ vs T^{-1} are linear, leading to an activation energy of 1.7 kcal mol⁻¹ and a preexponential factor of $1.4 (5) \times 10^7 \text{ s}^{-1}$ for the enhanced triplet decay process (Table II).

The transient kinetics exhibit a somewhat different profile when probing at 675 nm following laser excitation of Ru(III)–Zn-cyt

(21) (a) The nonzero asymptotes in the triplet decay probably arise from a small amount of irreversible photochemistry (<10%) induced by the laser excitation pulse. (b) The nonzero transient decays in parts b and c of Figure 1 arise both from irreversible photochemistry and from a small amount of unmodified protein that was not removed in the purification procedures.

(22) No luminescence has been reported for Ru(NH₃)₅L³⁺ complexes, and the excited-state lifetimes are expected to be at least as short as those of the d⁶ Ru(II) analogues.^{20b}

(23) Ford, P.; Rudd, De F. P.; Gaunder, R.; Taube, H. *J. Am. Chem. Soc.* **1968**, *90*, 1187–1194.

Table II. Observed and Calculated Rate Constants and Activation Parameters for the Ru–M–Cyt *c* Intraprotein Electron-Transfer Reactions

no.	reaction	$-\Delta G^\circ$, eV	k_{obsd} (298 K), s^{-1}	E_a (obsd), kcal mol $^{-1}$	$\Delta S^\ddagger_{\text{obsd}}$, ^a eu	k_{calcd} (298 K), s^{-1} , with λ , eV/ β , \AA^{-1}		
						1.85/1.2	1.5/1.5	1.2/1.8
7	Ru(II) \rightarrow Fe(III)-cyt c^b	0.18 (1)	$(3-5) \times 10^1$	2.1-4	-46 to -39	1.1×10^2	2.2×10^2	2.8×10^2
8	Ru(II) \rightarrow Zn-cyt c^*	0.36 (10)	$2.4 (1) \times 10^2$	2.2 (2)	-41 (2)	2.1×10^3	3.9×10^3	4.3×10^3
9	Ru(II) \rightarrow Zn-cyt c^{*+}	0.82 (10)	$1.6 (4) \times 10^6$			9.6×10^5	9.1×10^5	4.1×10^5
10	Zn-cyt $c^* \rightarrow$ Ru(III)	0.88 (10)	$7.7 (2) \times 10^5$	1.7 (2)	-27 (1)	1.8×10^6	1.5×10^6	5.7×10^5
11	Zn-cyt c^{*-} \rightarrow Ru(III)	1.38 (10)				8.1×10^7	1.7×10^7	1.0×10^6

^a ΔS^\ddagger defined in Table I. ^b References 7c and 8b.

c (Figure 1c). Due to the small magnitude of this signal, the decay curve shown in Figure 1c is an average of 250 laser shots. The rise of transient absorption at 675 nm is not "instantaneous" as it appeared to be at 450 nm²⁴ but instead grows in on a slower time scale and then decays with a first-order rate constant quite close to that measured at 450 nm. This kinetic behavior is consistent with an A to B to C reaction in which the rate constant for the B to C step exceeds that for the A to B reaction.²⁵ As in the bimolecular quenching experiments, any product formation must arise from electron transfer, though energy transfer could still contribute to the enhanced triplet decay. In the flash transient experiment, A would correspond to the Zn-porphyrin triplet, B, to the radical cation, and C, to the neutral ground-state Zn-porphyrin. A nonlinear least-squares fit of the 675-nm data to a five-parameter biexponential decay function appears in Figure 1c (smooth curve).²⁶ The coefficients of the two exponentials in the fit were used to estimate the yield of Ru(II)-Zn-cyt c^{*+} arising from triplet quenching. The calculated yield is 0.4 (3), but the considerable uncertainties that accumulate when extracting this yield from the fit parameters,²⁷ and the low probability of energy-transfer quenching,²⁸ suggest that the actual yield of electron-transfer products is probably close to 100%. The rate constant for the Zn-porphyrin* to Ru(III) electron-transfer reaction will therefore be taken as $7.7 (2) \times 10^5 s^{-1}$. The best fit obtained for the back-reaction rate constant was $1.6 (4) \times 10^6 s^{-1}$.

The Ru(NH₃)₅(His-33)³⁺ residue of the derivatized Zn-cyt *c* can be reduced to the Ru(II) state under an atmosphere of H₂ gas in the presence of some Pt gauze. The triplet state of Ru(II)-Zn-cyt *c* differs from those of both Zn-cyt *c* and the Ru(III) derivative, decaying with a rate constant of 305 (5) s⁻¹ at 25 °C. Evidently a new triplet-state decay pathway is present in Ru(II)-Zn-cyt *c* that does not appear in the unmodified protein and that has a rate constant of $2.4 (1) \times 10^2 s^{-1}$ at room temperature. The activation parameters for this decay process, listed in Table II, reveal a weak temperature dependence and a small preexponential factor.

It is more difficult to rule out energy transfer as the quenching mechanism in Ru(II)-Zn-cyt c^* . In this case, bimolecular quenching results have not been obtained nor was any evidence of a back-electron-transfer reaction uncovered. Rough estimates place the potential energy minima of the lowest lying triplets in Ru(II)-ammine complexes in the vicinity of 2.05 (25) eV,^{20b} slightly above the energy of the Zn-cyt *c* triplet. Even if the lowest energy triplet in Ru(NH₃)₅(His)²⁺ lies at the lower end of the

Table III. Estimated Half-Cell Potentials for Zn-Cyt *c*, Its Triplet Excited State, and Ru(NH₃)₅L^{3+/2+}, vs NHE, at 298 K

redox couple	E° , V	redox couple	E° , V
Fe ^{III/II} -cyt c^a	0.260 (2)	Zn-cyt $c^{*/-}$	0.44 (10)
Zn-cyt $c^{*+/0}$	0.9 (1)	Ru(NH ₃) ₆ ^{3+/2+}	0.060 (5)
Zn-cyt $c^{*+/*}$	-0.8 (1)	Ru(NH ₃) ₅ (His) ^{3+/2+} ^a	0.080 (5)
Zn-cyt $c^{0/*-}$	-1.3 (1)		

^a Reference 7c. ^b Reference 33.

range for Ru(II)-ammine complexes, the spectral overlap of Zn-cyt *c* phosphorescence and Ru(NH₃)₅(His)²⁺ triplet absorption bands will be vanishingly small due to the weak molar absorbances of the Ru(II) complexes and the expected breadth of their absorption profiles. Electron transfer, therefore, is a more plausible quenching mechanism for the Ru(II)-Zn-cyt *c* triplet.

Discussion

The electrochemical potentials for the oxidation and reduction of Zn-cyt *c* have not been determined, and this leads to some uncertainty in estimating the free energy changes associated with the ground- and excited-state electron-transfer reactions of Zn-cyt *c*. These measurements are hampered in part by the poor electrode kinetics exhibited by cytochrome *c*³⁰ and in part by the instability of Zn-cyt c^{*+} , which appears to decompose in less than 1 s. Half-wave potentials have been measured, however, for a variety of Zn-porphyrins in solution.³¹ The average values of these potentials are shown in Table III. The excited-state potentials given in this table were generated by subtracting from the Zn-cyt $c^{*/0}$ potential and adding to the Zn-cyt $c^{0/*-}$ potential the value of the Zn-cyt *c* triplet-state energy (1.71 eV).^{14,32} Since the potentials for the Ru(NH₃)₆^{3+/2+} and Ru(NH₃)₅(His)^{3+/2+} couples are 0.06 and 0.08 V, respectively, vs NHE at room temperature,^{7c,33} electron-transfer is clearly a viable mechanism for quenching Zn-cyt c^* by both the Ru(III)- and Ru(II)-ammine complexes.

In the bimolecular reactions 1-6 listed in Table I, electron-transfer rate constants span 3 orders of magnitude (10^2 - $10^8 M^{-1} s^{-1}$). The Ru-Zn-cyt *c* kinetics, when used in conjunction with the Ru-Fe-cyt *c* data, provide four intramolecular electron-transfer reactions (7-10, Table II) in which the rate constant varies over a range of nearly 5 orders of magnitude (3×10^1 - $2 \times 10^6 s^{-1}$). These wide variations in rate are likely to arise in large part from the differences in free energy changes for the reactions.³⁴⁻³⁶ In the semiclassical theory of electron-transfer reactions, the bimolecular rate constant (*k*) depends, in the absence of diffusion control, on the free-energy change (ΔG°) for the process via eq 1-6.³⁶ The term K_A is the equilibrium constant for formation

(24) The sharp negative spike in Figure 1c is due to scattered fluorescence. The slow rise of the 675-nm transient signal is not likely to arise from instrument recovery since the triplet signal of Zn-cyt *c* at 675 nm does not exhibit a comparable temporal profile.

(25) Frost, A. A.; Pearson, R. G. *Kinetics and Mechanism*, 2nd ed.; Wiley: New York, 1961; pp 166-169.

(26) One parameter in the biexponential function, the triplet decay rate, was fixed equal to $7.7 \times 10^5 s^{-1}$ during the fitting procedure.

(27) The determination of the yield of Ru(II)-Zn-cyt c^{*+} that results from triplet quenching depends critically upon the magnitude of the transient absorbance at $t = 0$ which, due to the large fluorescence spike, is not known with great certainty. Electron-transfer quenching of the singlet state can also interfere with the yield calculation.

(28) The lowest lying ligand field excited state in Ru(NH₃)₆³⁺ (⁴T_{1g}) has been assigned a vertical transition energy of 2.85 eV,²⁹ which is over 1 eV higher in energy than Zn-cyt c^* . Therefore, even with substantial relaxation energy, the ⁴T_{1g} state is unlikely to fall below 1.71 eV.

(29) Navon, G.; Sutin, N. *Inorg. Chem.* **1974**, *13*, 2159-2164.

(30) Betso, S. R.; Klapper, M. H.; Anderson, L. B. *J. Am. Chem. Soc.* **1972**, *94*, 8197-8204.

(31) Felton, R. H. In *The Porphyrins*; Dolphin, D., Ed.; Academic: New York, 1978; Vol. V, Chapter 3, pp 58-67.

(32) (a) The potentials reported in Table III agree within error with those reported by McLendon et al.^{2b,32b} (b) Magner, E.; McLendon, G. L., to be submitted for publication.

(33) Yee, E. L.; Cave, R. J.; Guyer, K. L.; Tyma, P. D.; Weaver, M. J. *J. Am. Chem. Soc.* **1979**, *101*, 1131-1137.

(34) Marcus, R. A. *Annu. Rev. Phys. Chem.* **1964**, *15*, 155-196.

(35) Newton, M. D.; Sutin, N. *Annu. Rev. Phys. Chem.* **1984**, *35*, 437-480.

(36) Marcus, R. A.; Sutin, N. *Biochim. Biophys. Acta* **1985**, *811*, 265-322.

$$k = K_A k_{et} \quad (1)$$

$$K_A = \exp(-\Delta G_A/RT) = c_0 \exp(-w_R/RT) \quad (2)$$

$$k_{et} = \nu \kappa \exp(-\Delta G_r^*/RT) \quad (3)$$

$$\Delta G_r^* = \lambda/4(1 + \Delta G^{\circ'}/\lambda)^2 \quad (4)$$

$$\lambda = \lambda_i + \lambda_o \quad (5)$$

$$\Delta G^{\circ'} = \Delta G^{\circ} + w_p - w_R \quad (6)$$

of the electron-transfer precursor complex in which the redox pairs are separated by a distance r ; ΔG_A is the free energy change associated with formation of the precursor complex, and one component of this free energy change is the electrostatic work, w_R , required to bring the reactants to separation r . The term k_{et} is the first-order rate constant for electron transfer within this precursor complex; ν is an appropriate frequency factor for motion along the reaction coordinate and will be taken to be independent of temperature and equal to $1 \times 10^{13} \text{ s}^{-1}$; κ is the electronic transmission coefficient for the reaction and is a function of the separation and orientation of the redox pairs; and ΔG_r^* is the activation free energy for electron transfer at separation r . This activation free energy depends (eq 4–6) upon the free-energy change for the reaction (ΔG°), the electrostatic work required to assemble the reactants (w_R) and products (w_p) into the precursor complex, and the inner (λ_i) and outer (λ_o) shell reorganization energies. Throughout the remainder of the discussion it will be assumed that the work-corrected free energy changes ($\Delta G^{\circ'}$) can be approximated by the standard free energy changes (ΔG°).

In the ideal case, K_A , κ , and λ could be held constant and ΔG° would be varied. The variation in observed rate constants would then reveal the magnitudes of $K_A \kappa$ and λ . The situation for the bimolecular reactions in Table I is complicated by the K_A factor in eq 1. Though it can be argued that K_A is roughly the same for the reactions of $\text{Ru}(\text{NH}_3)_5\text{L}^{2+}$ ($\text{L} = \text{NH}_3, \text{His}$) with $\text{Fe}^{\text{III}}\text{-cyt } c$ and $\text{Zn-cyt } c^{*+}$, the difference in the charges of the reactants is certain to change K_A for the quenching of $\text{Zn-cyt } c^*$ by $\text{Ru}(\text{NH}_3)_5\text{L}^{3+}$. Marcus and Sutin have estimated a value of 0.4 M^{-1} for K_A in the reaction between the $\text{Ru}(\text{II})$ complexes and $\text{Fe}^{\text{III}}\text{-cyt } c$,³⁶ and a similar value should suffice for the reaction with $\text{Zn-cyt } c^{*+}$. When the same Debye–Hückel model is used with different charges on the reactants, a calculation of the electrostatic work required to assemble the precursor complex leads to an estimate of 0.24 M^{-1} for K_A in the bimolecular $\text{Zn-cyt } c^*$ quenching reactions. Thus, the rate constants for oxidative quenching of $\text{Zn-cyt } c^*$ should be multiplied by $1.7 (=0.4/0.24)$ to put them on approximately equal footing (in terms of K_A) with the reactions in which an electron is transferred to $\text{M-cyt } c$. A further complication in these bimolecular reactions is a steric factor S , introduced to account for the greater probability of electron transfer at the exposed heme edge in $\text{M-cyt } c$. The factor S is multiplied by K_A to give an effective equilibrium constant for precursor complex formation, K_A' .³⁶ It is clear from eq 1–3 that $\ln k_{\text{obsd}}$ should be a linear function of ΔG_r^* with an intercept of $\ln(\nu \kappa K_A')$. The difference between $\ln k_{\text{obsd}}$ for any pair of reactions can be used to estimate λ , and a value of 1.2 eV is consistent with the bimolecular kinetics. The magnitude of $\ln(\nu \kappa K_A')$ can then be estimated to be -10.1 for these reactions. The rate constants calculated for reactions 1–6 with these parameters appear in Table I, and it can be seen that they agree to within a factor of 10 with the experimental rate constants.

More fundamental information can be obtained from the intramolecular electron-transfer kinetics because $\ln(SK_A) = 0$, leaving just λ and κ to be extracted from the experimental rate constants. The distance-dependent electronic transmission coefficient, κ , is frequently given by eq 7.³⁶ The redox partner

$$\kappa = \exp[-\beta(r - r_o)] \quad (7)$$

separation, r , will be taken as an edge-to-edge distance. In $\text{Ru-Fe-cyt } c$ this distance was assigned to the shortest separation between aromatic carbon atoms on His-18 and His-33 (11.8 \AA),^{7c} and the same value will be used for $\text{Ru-Zn-cyt } c$. The term r_o

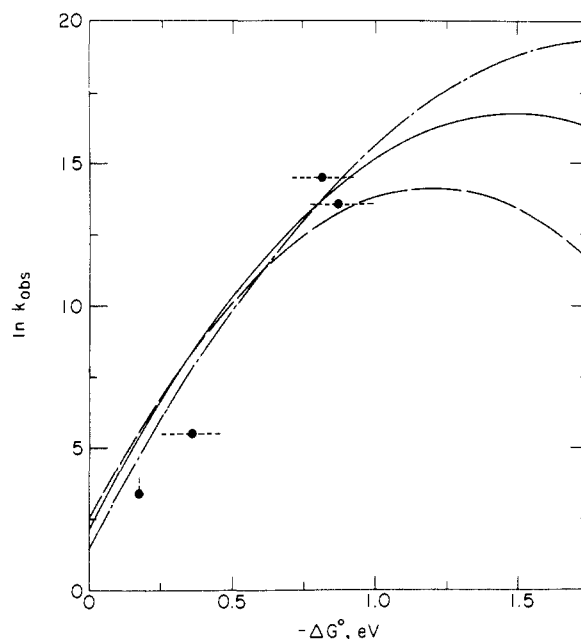


Figure 3. Plot of $\ln k_{\text{obsd}}$ vs $-\Delta G^{\circ}$ for the $\text{Ru-M-cyt } c$ ($\text{M} = \text{Fe}, \text{Zn}$) intraprotein electron-transfer reactions. Calculated curves: (---) $\lambda = 1.2 \text{ eV}$, $\beta = 1.8 \text{ \AA}^{-1}$; (-.-) $\lambda = 1.85 \text{ eV}$, $\beta = 1.2 \text{ \AA}^{-1}$; (—) $\lambda = 1.5 \text{ eV}$, $\beta = 1.5 \text{ \AA}^{-1}$.

is defined as the largest value of r at which the reaction is adiabatic ($\kappa = 1$).³⁶ The value of r_o will be different from zero because of the extension of electronic orbitals beyond the atomic nuclei and, following Marcus and Sutin, will be taken as 3 \AA .³⁶ Values of β in the range of $0.9\text{--}1.2 \text{ \AA}^{-1}$ have emerged from studies of long-distance electron transfer in rigid glasses,³⁷ and fixed-site electron-transfer reactions in Ru -modified Zn -myoglobin.¹³

Since ΔG_r^* depends quadratically upon ΔG° , a plot of $\ln k_{\text{obsd}}$ vs ΔG° for a homologous series of fixed-site electron-transfer reactions with constant λ and κ should be parabolic with a maximum at $-\Delta G^{\circ} = \lambda$. The intramolecular electron-transfer data for $\text{Ru-M-cyt } c$ are represented by such a plot in Figure 3. If λ is assigned the value obtained from the bimolecular electron-transfer reactions (1.2 eV), then a value of $\beta = 1.8 \text{ \AA}^{-1}$ is necessary for reasonable agreement with the data (dashed curve, Figure 3). These parameters tend to overestimate the rates of the lower driving-force reactions and underestimate the higher driving-force processes (Table II), and the value of $\beta = 1.8 \text{ \AA}^{-1}$ is somewhat larger than most other estimates of this parameter.^{13,36,37} That the ratio of the rate constants for reactions 10 and 7 is a factor of 90 greater than the ratio for reactions 6 and 2 suggests that a larger value of λ might be appropriate for the intramolecular reactions. Good agreement with the $\ln k_{\text{obsd}}$ data results with $\lambda = 1.85 \text{ eV}$ and $\beta = 1.2 \text{ \AA}^{-1}$ (dot-dashed curve, Figure 3; Table II). This value of λ is somewhat larger than expected³⁶ and does not yield the best predictions of activation parameters (vide infra). The intermediate values of $\lambda = 1.5 \text{ eV}$ and $\beta = 1.5 \text{ \AA}^{-1}$ produce the solid curve in Figure 3, and the calculated rate constants agree with experiment to within about a factor of 10 (Table II).

All of the electron-transfer reactions described above exhibit relatively mild temperature dependences over the $5\text{--}40 \text{ }^{\circ}\text{C}$ range (Table II). Marcus and Sutin have explained the small enthalpy of activation for the $\text{Ru}(\text{II})$ to $\text{Fe}(\text{III})$ intramolecular electron transfer in terms of the large negative enthalpy change associated with the reaction.³⁶ It is important to note that the best agreement between the calculated and experimental activation parameters for $\text{Ru-Fe-cyt } c$ results with the values $\lambda = 1.2 \text{ eV}$ and $\beta = 1.8 \text{ \AA}^{-1}$. Thermodynamic parameters are not yet available for the $\text{Ru-Zn-cyt } c$ electron-transfer reactions so an identical analysis

(37) Miller, J. R.; Beitz, J. V.; Huddleston, R. K. *J. Am. Chem. Soc.* **1984**, *106*, 5057–5068.

of the activation parameters cannot be applied.

The foregoing analysis demonstrates that, in order to define the reorganization energy (λ) and electronic transmission coefficient (κ) for a homologous series of intramolecular electron-transfer reactions, rate constants must be acquired for reactions that span a wide range of ΔG° values, especially those in the neighborhood of $-\Delta G^\circ = \lambda$.³⁸ These strict requirements can be relaxed somewhat if activation parameters and accurate thermodynamic parameters are available. In the absence of such a complete data base, λ and κ (or β) can only be confined to specific ranges of values. In the present case, estimates of λ for the Ru-M-cyt *c* fixed-site electron-transfer reactions range from 1.2 to 1.85 eV. Though $\lambda = 1.2$ eV adequately describes the bimolecular reactions,³⁹ this reorganization energy must be coupled with an unusually large β in order to accurately predict the intramolecular rate constants. Gray's work on ruthenium-modified Zn-myoglobin,¹³ however, suggests that $\beta = 1.0$ (1) Å⁻¹ for the Zn-porphyrin* to Ru(NH₃)₅(His)³⁺ intraprotein electron transfers. Accepting this value of β implies that a larger value of λ is required for the Ru-M-cyt *c* reactions. This is not inconsistent with the large outer-sphere reorganization energies expected for long-distance electron transfers in spherical or ellipsoidal cavities.⁴⁰ It is clear from Figure 3 that in order to refine these electron-transfer parameters, rate constants must be measured for reactions with greater thermodynamic driving force. If the rate constants for more exergonic processes are much greater than 10⁶ s⁻¹, then the larger values of λ are indicated. Alternatively, if the rates reach a plateau in the vicinity of (1–5) × 10⁶ s⁻¹, then the smaller λ and larger β would be appropriate.

Another complication can arise from protein conformational changes associated with the electron-transfer reactions. It has

(38) Implicit in the analysis of the intraprotein electron transfers is the assumption that ΔG° is the only variable among the four reactions studied thus far. The inconstancy of κ (or τ) or λ for these reactions will lead to deviations of experimental points from the "best fit". Many more reactions with widely varying values of ΔG° must be studied before the assumption of constant κ and λ can be confirmed.

(39) The rate constants for the faster bimolecular reactions are probably approaching the diffusion limit (ca. 5×10^9 M⁻¹ s⁻¹).³⁶ The purely activation-controlled rate constants would then be expected to be slightly greater than the observed rate constants, leading to a somewhat larger estimate for λ . This correction, however, is relatively minor and is not likely to fully account for the apparent differences in λ between the bimolecular and intramolecular electron-transfer reactions.

(40) Brunschwig, B. S.; Ehrenson, S.; Sutin, N. *J. Phys. Chem.* **1986**, *90*, 3657–3668.

been reported recently that the rate constant for an Fe(II) to Ru(NH₃)₄(isonicotinamide)(His-33)³⁺ electron transfer is less than 10⁻³ s⁻¹ ($\Delta G^\circ = -0.18$ eV).¹¹ The unusually slow electron-transfer rate has been attributed to a conformational change of the Ru(III)-Fe(II)-cyt *c* species into a configuration that inhibits electron transfer. The correlation of rate constants with ΔG° represented in Figure 3, however, suggests that the 30 s⁻¹ rate constant for the Ru(II) to Fe(III) intraprotein electron transfer in Ru(NH₃)₅(His-33)-Fe-cyt *c* is not limited by a protein conformational change. It is possible, however, that the conformational dynamics of cyt *c* are responsible for some of the deviations of calculated values from the experimental kinetics parameters in the Ru-M-cyt electron-transfer reactions.

Summary

The rates of intraprotein electron transfer in Ru-M-cyt *c* (M = Fe, Zn) exhibit a dependence on ΔG° that is consistent with the predictions of the semiclassical theory of electron transfer. The rate constants for these processes span more than 4 orders of magnitude over a 0.7-eV change in driving force. The best estimates of reorganization energies and distance dependence are $\lambda = 1.2$ –1.85 eV and $\beta = 1.2$ –1.8 Å⁻¹. These estimates can be improved by measuring the rates of analogous reactions with larger driving forces and by refining the values of the thermodynamic parameters for the various electron-transfer processes. Experiments along these lines are in progress.

Acknowledgment. We are very grateful to Dr. Norman Sutin for many valuable discussions and suggestions during the course of this work. We also thank Professor Harry B. Gray for several helpful discussions and for providing a preprint of ref 13. We acknowledge Professors Daniel G. Nocera and George L. McLendon for their contributions during the early stages of this project and Elinor Norton for performing the atomic absorption spectroscopic analyses. This work was performed at Brookhaven National Laboratory under Contract DE-AC02-76CH00016 with the U.S. Department of Energy and supported by its Division of Chemical Sciences, Office of Basic Energy Sciences.

Supplementary Material Available: Reversed-phase HPLC of tryptic digestion fragments of native and modified cytochromes (Figure 1, Fe-cyt *c* and Zn-cyt *c*; Figure 2, Zn-cyt *c* and Ru-Zn-cyt *c*) and absorption spectra of Ru(NH₃)₅(His)³⁺ and Ru-containing tryptic digestion fragment from Ru-Zn-cyt *c* (Figure 3) (3 pages). Ordering information is given on any current masthead page.